RSC Advances

PAPER

View Article Online
View Journal | View Issue

Cite this: *RSC Adv.*, 2026, **16**, 5206

Synergistic effects of poly-silicon aluminum sulfate and auxiliary agents in dye wastewater decolorization

Jie Min,[a] Huilan Zhou,[a] Chao Yang,[a] Lu Wang,[a] Jiajun Nie,[b] Qiang Wang,[b] Lijun Wang[b] and Yunlong Zhao *[a]

Herein, the color-removal effectiveness of nine different structured dyes was compared using self-synthesized poly-silicon aluminum sulfate (PSAS) and six commercial coagulants, namely aluminum sulfate (Alum), polymerized ferric sulfate (PFS), magnesium sulfate ($MgSO_4$), polymerized aluminum chloride (PAC), poly-dimethyl-diallyl-ammonium chloride (PAMDAAC) and anionic-polyacrylamide (APAM). The inorganic polymer coagulants (PAC and PSAS) showed different advantages in the coagulation process. In particular, the latter was adaptable to a wide pH range and exhibited high decolorization ability for most dyes. The color-removal rate of five dyes (two direct dyes, one disperse dye and two acid blue dyes) reached over 90% at a pH of 11. The decolorization efficiencies of reactive black 5 and reactive blue 21 dyes were relatively poor at 40.87% and 75%, respectively. However, none of the seven coagulants could achieve a satisfactory effect on the cationic dyes with stable structures. Most non-cationic dyes have the $R-SO_3^-$ group, which could combine with the Al polymer or Al^{3+} in the coagulant to achieve varying degrees of dye removal. These findings were further supported by FTIR analysis. Zeta-potential analysis indicated that the decolorization of dye wastewater using PSAS was based on a charge neutralization process. Further, four kinds of auxiliaries were used to remove basic dyes. Among them, phosphomolybdic acid (PMoA) showed good performance. With a dosage of 100 mg L^{-1} PMoA and 50 mg L^{-1} PSAS, the decolorization rate of rhodamine B (https://www.chembk.com/en/chem/Rhodamine_B) reached 94.2%. Finally, the nine pure dyes were mixed in a 1 : 1 ratio to prepare mixed-dye wastewater with a total concentration of 100 mg L^{-1}. The removal rate was 25.3% using PSAS. However, in the presence of PMoA, the removal rate reached 92.5%. Therefore, the combined PMoA and PSAS technology can also achieve desirable results for treating such wastewater.

Received 26th August 2025
Accepted 7th January 2026

DOI: 10.1039/d5ra06377a

rsc.li/rsc-advances

1. Introduction

Synthetic dyes are widely used in the textile, paper, tanning, pharmaceutical, plastic, and food-processing industries because of their coloring properties, production ease and high production speed.[1] Based on available data, various pigments used commercially in dyes have reached 700 000 tons per year.[2] Notably, a significant portion (10–15%) of dyes ultimately end up in wastewater due to process inefficiencies. This effluent possesses typical characteristics such as deep coloration, high organic load, complex composition, significant chemical oxygen demand (COD), and low biodegradability, thereby rendering it a notoriously difficult category of hazardous industrial wastewater to treat.[3] Synthetic dyes are one of the most common sources of pollution in wastewater, as they are toxic and carcinogenic, thereby posing a significant threat to human health and the survival of terrestrial and marine life.[4] Therefore, an efficient, non-toxic, and low-cost technique is essential for treating dye wastewater.[5]

The treatment of textile wastewater is notably challenging, primarily due to the substantial variability in dye types used and the inherent stability of many dyestuffs against photo-degradation and oxidation. This has posed a significant challenge to the adsorption and degradation treatment technology of dyes. Thus, a reasonable choice of technology based on the difficulties of this technique is exceedingly necessary. Various methods have been developed to remove dyestuffs from textile wastewater, employing physical, biological, and chemical processes, among others.[6] These processes are subdivided into the following technologies: adsorption,[7] photo-catalytic degradation,[8] ion exchange,[9] membrane technology,[10] biological–chemical processes,[11] aerobic and anaerobic processes,[12] oxidation and Fenton processes[13] and coagulation–flocculation.[14,15] Due to the strong adsorption of activated sludge on

[a]*Key Laboratory of Oil & Gas Fine Chemicals, Ministry of Education, Xinjiang Uyghur Autonomous Region, School of Chemical Engineering and Technology, Xinjiang University, Urumqi 830046, China. E-mail: zhaoyunlong908@xju.edu.cn*
[b]*Xinjiang Huier Agricultural Group Co., Ltd, Department of Technology Research and Development, Changji, 831100, China*

dyes, the conventional biological treatment process is largely effective in treating suspended matter, BOD and color. However, the use of this process is limited by its long treatment time, the large required operating space, and the toxicity and recalcitrance of dyes.[16] Adsorbents have a high color removal rate and strong regeneration capacity.[7,17,18] However, considering the amount of sludge generated and the high cost of adsorbent recovery, alternative methods are often considered. Electrochemical advanced oxidation, which is based on the oxidation of OH radicals, is effective for treating unsaturated and saturated compounds.[19] Its disadvantages include low stability and high operating costs. However, flocculation and coagulation are not only relatively mature technologies but have few rivals in terms of treatment capacity and timeliness.

The complexity of actual industrial textile wastewater is unimaginable. Usually, its treatment process is a hybrid/combination process. Coagulation is part of the combined treatment process; its importance as a pre-treatment technology for water treatment cannot be overstated.[20] Moreover, the core of the coagulation technology is the research and use of coagulants. Various types of coagulants have been developed and used, such as common aluminum and iron salts, PAC, PFS, PSAS, and organic coagulants.[21] However, there is an absence of a systematic evaluation and comparison of the performance of different types of coagulants for the treatment of various types of dye wastewater. Here, we compare the color removal performance of a homemade PSAS coagulant using the sol method with six widely commercially available agents ($Al_2(SO_4)_3$, PFS, $MgSO_4$, PAC, PAMDAAC and APAM). Seven coagulants are studied for the decolorization treatment of nine dyes. The nine dyes are of five types: direct, disperse, reactive, acid and cationic dyes (basic dyes). Among them, the cationic dyes contain very complex aromatic groups that are difficult to biodegrade and remove. Most of the current coagulation methods for removing basic dyes require organic coagulants. Felix Mcyotto's study shows that the color removal rate of alkaline crystalline violet using the anionic coagulant polyacrylamide is only 5.3%.[22] Khai Ern Lee *et al.* have employed an aluminum sulfate–aloe vera hybrid coagulant to remove methylene blue, achieving a maximum removal efficiency of 70%.[23] However, their color removal effect is also unsatisfactory. Yang has used Ca^{2+} in calcium dodecyl sulfate to generate tiny precipitates with methylene blue, which are then removed by flocculation with microbial flocculant GA1.[24] The color removal rate of the dyes reaches up to 98.6%. However, the method also has its limitations, especially its unclear effectiveness for other types of dye treatment. In summary, one thing is confirmed: flocculation and coagulation techniques are still generally accepted and widely used today. The effective treatment of basic dyes has historically been a challenge. It is even more difficult to treat mixed dyestuffs (mixed-dye wastewater of the 5 types of dye mentioned above). There is an urgent need for a universal technology to treat mixed-dye wastewater.

Here, nine types of dye wastewater are treated using the PSAS coagulant synthesized by the sol method (pre-synthesized inorganic polymer coagulant). A comparative study with the performance of other coagulants is also conducted. Subsequently, a suitable auxiliary is selected for the treatment of the basic dye wastewater. Infrared and zeta-potential are utilized to analyze the coagulation mechanism of PSAS on the dye wastewater. Finally, the PSAS coagulant and additives are used to treat the mixed dye wastewater, and the desired results are obtained.

2. Materials and methods

2.1 Materials

The nine dyes used in this experiment were Congo red dye (direct red 28), direct lake blue-5B, disperse red 167, acid red 27, acid blue 93, reactive black 5, reactive blue 21, basic violet 10, and basic blue 9. The main chromophore of the dyes and the maximum absorption wavelength are shown in Table 1.

The seven coagulants used for the experiments were self-synthesized poly-silicate aluminum sulfate (PSAS), aluminum sulfate (Alum), polymerized ferric sulfate (PFS), magnesium sulfate ($MgSO_4$), polymerized aluminum chloride (PAC), poly-dimethyl-diallyl-ammonium chloride (PAMDAAC), and anionic polyacrylamide (APAM). In the subsequent decolorization experiments, the dosages of coagulants PSAS, PFS, PAC, and $MgSO_4$ were calculated and expressed based on the mass of their respective key metallic elements: aluminum (Al), iron (Fe), and magnesium (Mg), in milligrams per liter (mg L^{-1}). Further, PAMD and APAM were counted in mg L^{-1}. The four auxiliary decolorizers were kaolin (KC), starch (SC), ammonium molybdate (AMo) and phosphomolybdic acid hydrate (PMoA), which were purchased from Sinopharm Chemical Reagent Co., Ltd.

2.2 Experimental procedure

2.2.1 Preparation of the PSAS coagulant. Here is a brief description of the synthesis of the PSAS coagulant by the sol method. Small amounts of a stabilizer and sodium aluminate were mixed and dissolved in quantitative deionized water. After boiling the above mixed liquid and cooling to ambient temperature, a clarified solution (1 mol L^{-1}) was obtained. Then, the solution was diluted to 5 wt% (SiO_2 wt%) water glass solution, which was added to sodium aluminate to obtain a silica aluminum sol precursor. Then, the precursor was slowly added to a 0.8 mol L^{-1} $Al_2(SO_4)_3$ solution prepared in advance at a stirring rate of 500 rpm. The obtained translucent suspension was stirred for 0.5 h. Thereafter, it was digested at 75 °C for 2 h. After polymerization for 2 h, a clarified solution of the PSAS coagulant was successfully obtained.[25]

2.2.2 Coagulation experiments. By adding 1 g of dye to 10 L of deionized water and stirring thoroughly, 100 mg L^{-1} of dye wastewater was obtained. A classical six-link stirring experiment was performed by adding 500 mL of the simulated dye wastewater to a stirring beaker. The initial pH of the dye wastewater was adjusted to the desired value using 0.1–1 mol L^{-1} NaOH and H_2SO_4 solutions. A specific amount of coagulant was then added to the stirring beaker; the mixture was stirred rapidly at 300 rpm for 2 min, stirred slowly at 60 rpm for 10 min, and then allowed to settle for 30 min. Subsequently, water samples were collected with a dropper at 2 cm below the liquid surface, and

Table 1 Dye characteristics–chromophoric group and maximum absorbance wavelength

Name of dyes	Chromophoric group	λ_{max} (nm)
Disperse red 167	Azo	459
Direct red 28 (Congo red)	Azo	498
Direct turquoise blue 5B (https://www.chembk.com/en/chem/Direct Turquoise Blue 5B)	Azo	600
Acid blue 93	Triarylmethane	630
Acid red 27	Azo	511
Reactive black 5	Azo	620
Reactive blue 21	Phthalocyanine	220
Basic blue 9 (methylthioninium chloride)	Xanthene	663.5
Basic violet 10 (rhodamine B)	Triarylmethane	553

their absorbance at λ_{max} was measured. The color removal efficiency was calculated as follows.

$$\text{Color removal efficiency } \eta\% = (C_0 - C_t)/C_0 \times 100, \quad (1)$$

where C_0 is the initial concentration of the dye wastewater, and C_t is the supernatant concentration in the treated dye test solutions. Deionized water was used as a blank reference.

2.2.3 Coagulation decolorization of the mixed dyes. Initially, 1.11 L of each of the nine dyestuffs mentioned above was taken and mixed to obtain 10 L of mixed-dye wastewater with a known total concentration of 100 mg L^{-1}. The concentration of each dye in the mixed-dye wastewater was 11.11 mg L^{-1}. Afterward, 500 mL of the mixed-dye wastewater was added to a 1000 mL stirring beaker, and then, its pH value was adjusted with dilute NaOH solution. PMoA (Mo: 100 mg L^{-1}) was added, followed by the dropwise addition of the PSAS coagulant (50 mg L^{-1}, calculated as Al mg L^{-1}). The subsequent coagulation experiments employed the same conditions and methods as described in the preceding section.

2.3 Analysis and testing instruments

The flocs produced by the coagulation of PSAS with dyes were freeze-dried. The resulting solid powders were analyzed for their phase composition using a Rigaku TTRIII X-ray diffractometer manufactured by Rigaku, Japan (XRD test parameters: angles of 10–80°, rate of 10° min^{-1}). The powder sample morphology was observed using SEM (JSM-6360LV) technology, which was manufactured by Nippon Electron Co. The powder samples were pressed using potassium bromide as the masterbatch, and their infrared spectra were measured using a Nissan Hitachi 270–30 infrared spectrometer. Zeta potential measurements were performed using a Zano-ZS potential distribution analyzer, which was acquired from Malvern Instruments, UK. The absorbance of the solutions was measured using a UV-vis spectrophotometer, UV-2450PC. The ICP technique was used for the determination of elemental phosphorus in wastewater.

3. Results and discussion

3.1 Effect of pH and coagulant type on the color removal rate of dyes

3.1.1 Effect of the pH and coagulant type on the color removal rate of azo-structured dyes. For the coagulation process, pH is an important factor and usually becomes the focus of research. For this study, the coagulant dosage is an overdose of 100 mg L^{-1}.[22] The effects of the initial pH on the coagulation color removal of azo-structured dye wastewater were studied using seven different coagulants, as shown in Fig. 1.

Fig. 1(a) and (b) show the removal efficiencies of direct red 28 and direct lake blue 5B, respectively. At a pH of 11, PSAS achieved 98.4% decolorization of the Congo red dye, which was slightly less than that of PAC (98.6%). For the removal of direct lake blue 5B, the color removal efficiencies of these two coagulants were more than 98.7%. It was possible to draw another obvious conclusion that coagulants containing metal cations also had a better effect on the removal of direct dyes. Fig. 1(c) shows the effect of pH and the types of coagulant on the color removal efficiency of the disperse red 167 dye. At a pH value of 11, PAC had the best decolorization effect of 99.5% for the disperse dyes, followed by PSAS at 97.35%. The high salinity of PAC may contribute to its better net puff effect in the treatment of disperse red. When the initial pH was between 5 and 9, the performance of aluminum sulfate was lower than that of polymerized ferric sulfate. Since polymerized ferric sulfate is an inorganic polymer, its net fluttering effect is greater than that of aluminum sulfate. Disperse red 167 is a non-ionic dye; thus, the removal of this dye is attributed to the wrapping of the mesh structure after the hydrolysis of the coagulant. As shown in Fig. 1, PAC and PSAS exhibited higher removal efficiencies in decolorizing the azo-structured dyes compared to other coagulants. However, PSAS was less affected by the pH of the dye wastewater than PAC.

3.1.2 Effect of the pH and coagulant type on the color removal rate of non-azo-structured dyes. The effects of the initial pH of the dye wastewater and the type of coagulant on the decolorization of non-azo dyes are shown in Fig. 2.

From Fig. 2(a), it can be seen that PSAS shows better decolorization performance for acid blue 93 compared to other coagulants at a pH value of 11. However, PSAS did not have any color removal effect on basic violet 10, which had the same triarylmethane chromogenic group as acid blue 93 (Fig. 2(b)). The apparent difference in the color removal rate may be attributed to the auxochrome group. The auxochrome groups influence the electrical properties of the dye effluent, *i.e.*, the positive and negative potentials. An interesting phenomenon could be observed in the decolorization test of alkaline dyes. At an appropriate pH, the coagulant was added to the dye

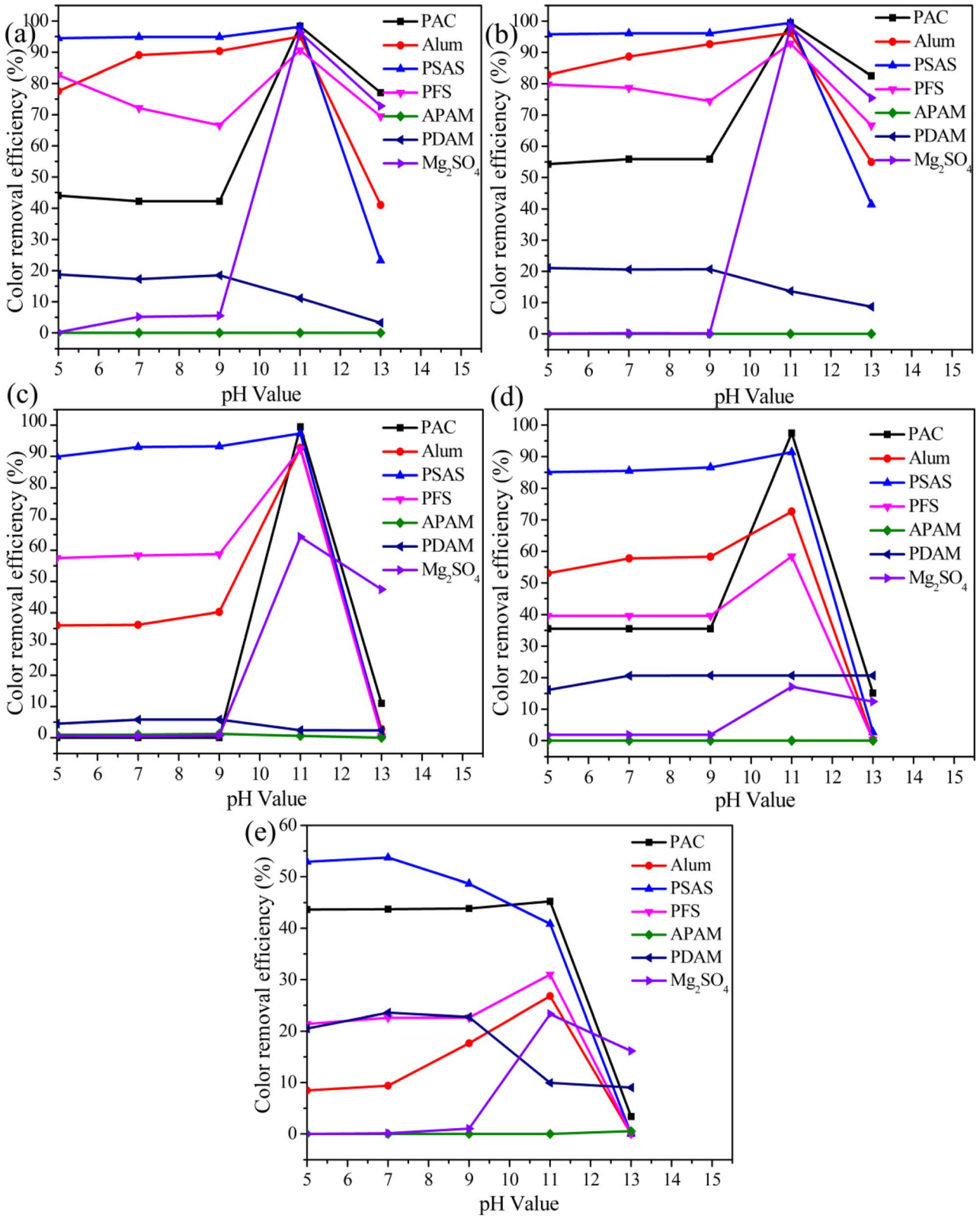

Fig. 1 Effect of the pH of the dye wastewater and coagulant type on the color removal rate of the azo-structured dyes; (a) Congo red or direct red 28, (b) direct lake blue 5B, (c) disperse red 167, (d) acid red 27 and (e) reactive black 5.

wastewater. Following coagulation and sedimentation, a substantial amount of flocs was observed to settle at the bottom of the beaker. However, the absorbance of the dye wastewater showed a negligible decrease. This result indicated that the basic violet 10 dye molecules did not undergo a chemical reaction with the coagulant. In other words, basic violet 10

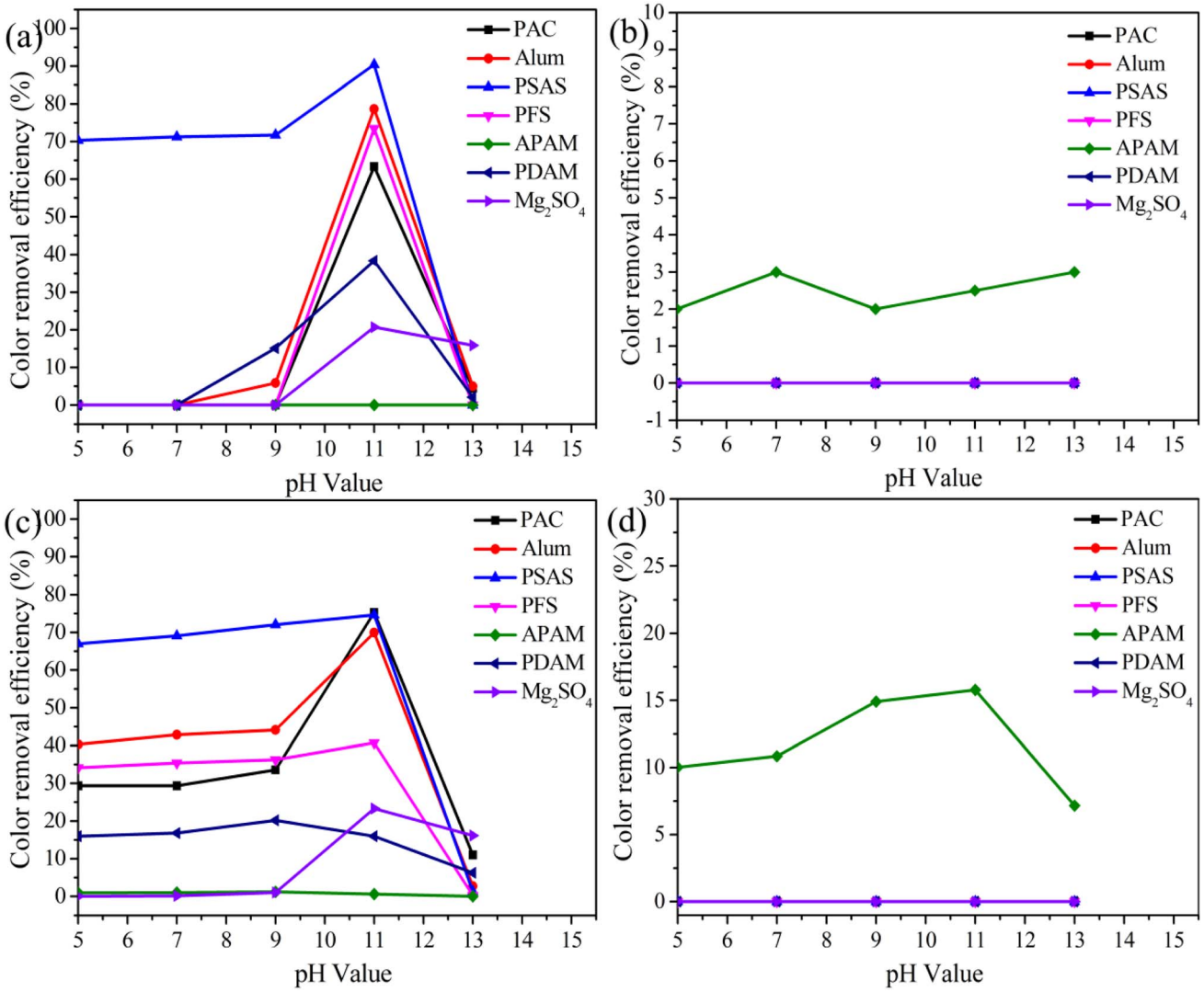

Fig. 2 Effect of the initial pH of the dye wastewater and coagulant type on the color removal rate of non-azo-structured dyes; (a) acid blue 93, (b) basic violet 10, (c) reactive blue 21 and (d) basic blue 9.

lacks a group (such as the $NaSO^{3-}$ group in acid blue 93) that interacts with metal cations. The anionic polyacrylamide coagulant proved partially effective for color removal; nevertheless, its overall performance was limited. Related studies have demonstrated that the coagulation process of anionic polyacrylamide with basic dyes is initiated by charge neutralization.[22] The aluminum-based coagulants exhibited high color removal rates for phthalocyanine dyes (reactive blue 21) (Fig. 2(c)). The result may be attributed to the properties of the aluminum salts. The color removal results for basic blue 93 were similar to those for basic violet 10 (Fig. 2(d)). The aforementioned experiments were conducted under conditions of sufficient coagulant dosages. The inorganic polymeric coagulants exhibited superior properties compared to other coagulants. However, the pH adaptability of aluminum chloride for water treatment was lower than that of PSAS. Therefore, the coagulation behavior of PSAS was investigated further.

3.2 Effect of the PSAS coagulant dose on the decolorization of dye wastewater

Here, the optimal amount of PSAS was determined at the aforementioned suitable pH. The PSAS coagulant dose varied from 0 to 200 mg L^{-1}, as depicted in Fig. 3. The overall removal effect of the dye wastewater treatment was less significant at a coagulant dose of 10 mg L^{-1}, resulting in low color uptake, likely due to the dissolved aluminum species. To clearly understand the coagulation process, it was necessary to analyze the pH of the supernatant after coagulation. The pH of this supernatant was approximately 10.5. Partial aluminum hydroxide precipitates dissolved to produce $Al(OH)_4^-$ at pH > 6.8.[26] With the increase in the coagulant dose, the pH of the dye wastewater showed a decreasing trend. At this stage, the effect of the PSAS coagulant on color removal became more pronounced. The color uptake results indicated that the optimal dose of PSAS was 50 mg L^{-1}.

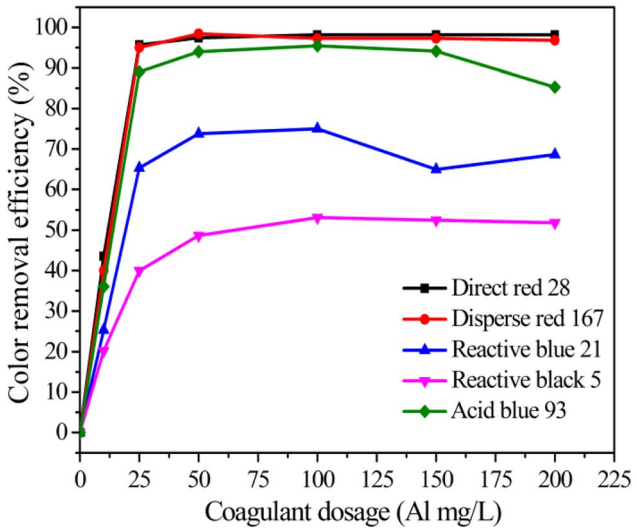

Fig. 3 Effect of the PSAS coagulant dose on the dye decolorization rate.

3.3 Effect of PSAS and additives on the decolorization of the basic dye wastewater

From the above experiments, it was clear that the six coagulants were ineffective or unsatisfactory in treating basic dyes (basic violet 10 and methylene blue). Ion-type analysis was conducted, revealing that both dyes were cationic in nature. However, aluminum and iron salt coagulants are also cationic. They have the same electrical properties as cationic dyes, *i.e.*, positively charged. The same type of charges repel each other, which is not conducive to the removal of basic dyes. Based on electrical properties, anionic polyacrylamide appears to be a good choice. However, its coagulation effect on basic dyes was unsatisfactory. In addition, the introduction of organic matter resulted in chemical oxygen demand (COD) or biochemical oxygen demand (BOD) for subsequent treatments. Consequently, more researchers are focusing on auxiliary agents.

In this study, we selected four additives for comparison. The additives were starch (100 mg L^{-1}), kaolin (100 mg L^{-1}, calculated as Al mg L^{-1}), ammonium molybdate and PMoA (Mo: 100 mg L^{-1}). As shown in Fig. 4(a), the dye wastewater color of basic violet 10 remained dark when only the other three additives (excluding PMoA) were added without coagulants. Additionally, its absorbance did not decrease at all. The color removal rate of basic violet 10 was 63.9% with PMoA. The use of this additive also had a significant effect on pH, with an optimal pH range around 9. However, we added PSAS to observe the results. The test results showed a satisfactory color removal rate of 97.1%, as seen in Fig. 4(c). For basic blue 9, both AM and PMoA demonstrated good color removal performance. This result was likely due to the action of molybdenum. As shown in Fig. 4(d), PSAS has a varying effect on the removal of the basic dye molecules using ammonium molybdate and PMoA. However, it was within the acceptable range. In this context, PSAS acted as an acid to some extent, broadening the pH range of the additive. Overall, PMoA was a more suitable agent for the removal of the basic dyes.

The use of PMoA will introduce phosphorus (P) into the treated wastewater. However, the residual phosphorus content in the discharged wastewater must meet stringent upper limit criteria. Therefore, the dosage of PMoA warrants careful consideration and study. The effect of the PMoA auxiliary dose on the decolorization rate of basic violet 10 in dye wastewater is shown in Fig. 5(a). As shown in Fig. 5(a), the color removal rate of basic violet 10 reached 97.1% at a PMoA auxiliary dose of 100 mg L^{-1}. However, continuing to increase the PMoA dose did not significantly change the decolorization effect of basic violet 10. However, the residual phosphorus concentration in the solution increased significantly with relatively high PMoA dosages. As shown in Fig. 5(b), at a PMoA dosage of 100 mg L^{-1}, the residual phosphorus concentration in the supernatant after coagulation was 0.52 mg L^{-1}, which was less than the 1 mg L^{-1} limit. Additionally, the phosphorus content in the wastewater met the discharge standard for water pollutants in the textile dyeing and finishing industry (GB4287-2012). The experimental results presented in Fig. 5 indicate that a PMoA dosage of 100–200 mg L^{-1} is safe and effective.

3.4 Enhanced color removal performance of PSAS for the mixed dye with PMoA

To determine the universality of the above joint operation process, we studied the decolorization performance of mixed dyes. The treatment of mixed-dye wastewater containing anionic, nonionic, and cationic dyes has rarely been reported. In this study, the nine dye wastewater mentioned above were mixed in a specific ratio. The changes in concentration and absorbance are shown in Fig. 6(a). As shown in Fig. 6(a), the maximum absorption peak of the mixed dyes was observed at 552–554 nm. The maximum absorption peak showed a consistent variation with the concentration. The fitted curve between concentration and absorbance is shown in Fig. 6(b). The R^2 value of the fitted equation was 0.9983, indicating a strong linear relationship. This indicated a linear relationship between absorbance and concentration changes. Initially, the PSAS coagulant was studied at a dose of 50 mg L^{-1}. The result was unsatisfactory, with a decolorization rate of only 25.3%, as indicated by the red line in Fig. 6(c). This was likely due to the interference of basic dyes with the coagulation effect of PSAS. However, when PMoA was added to the mixed dyes, the PSAS coagulant showed a significant color removal effect, with a removal rate of 92.5%. Furthermore, the chromaticity of the dye wastewater changed significantly. This is observed in Fig. 6(d). In the left glass vial shown in Fig. 6(d), it can be seen that the flocs produced by the mixed dyes and flocculants settle well at the bottom of the vial. The results demonstrated that the combined PMoA and PSAS technique was a highly effective approach for dye removal.

3.5 Discussion of the coagulation mechanism of PSAS

Currently, zeta potential analysis is an effective method to validate the theory of charge neutralization in coagulation processes. The zeta-potential changes during the coagulation process using PSAS to treat dye wastewater were measured and are shown in Fig. 7. As shown in Fig. 7(a), the initial zeta potential of the simulated Congo

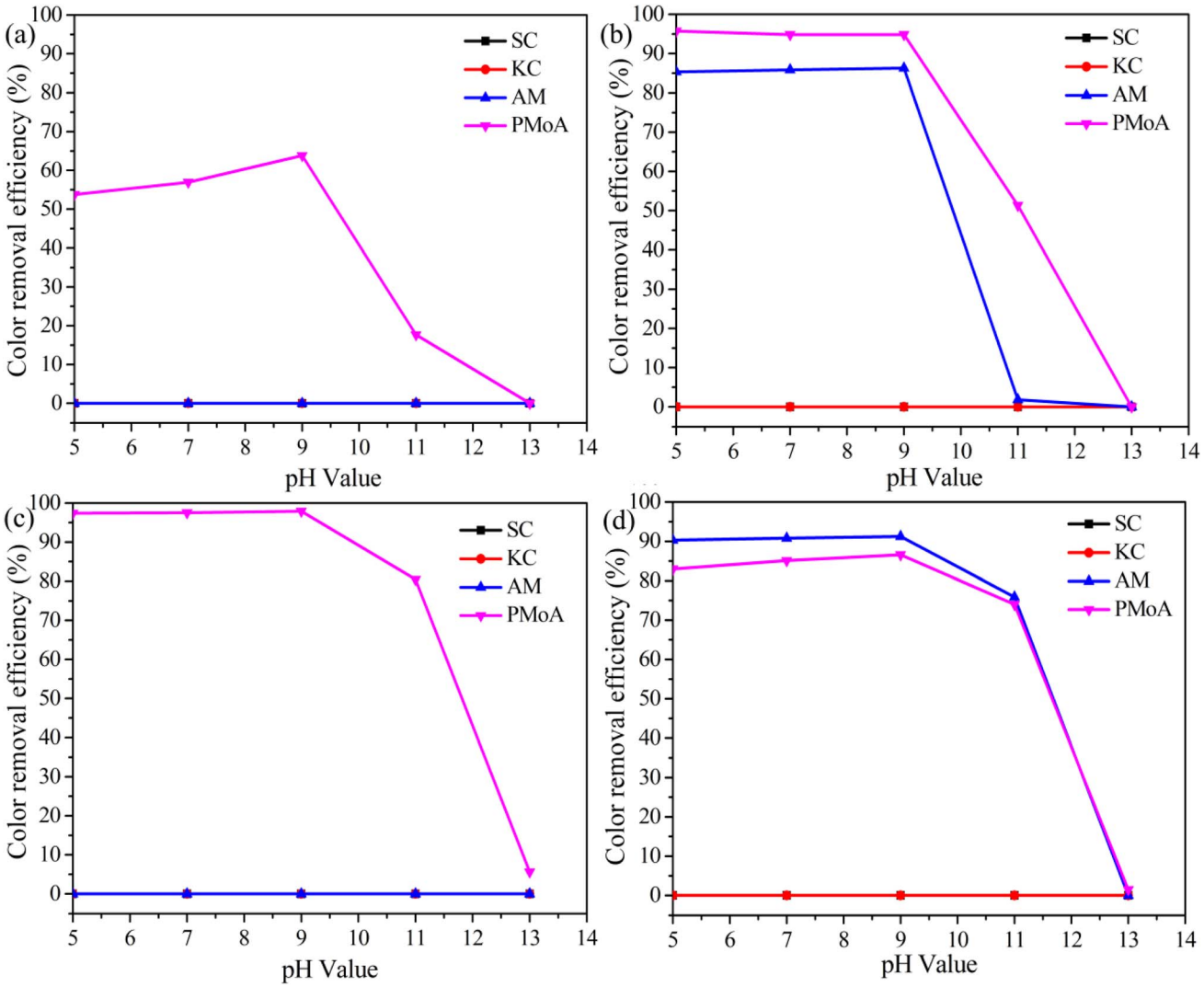

Fig. 4 Effect of different reagents and pH on the color removal rate of the dye wastewater: (a) basic violet 10 (without PSAS), (b) basic blue 93 (without PSAS), (c) basic violet 10 (added PSAS) and (d) basic blue 93 (added PSAS).

red dye wastewater at pH 11 is −13.2 mV. When 25 mg L^{-1} of PSAS coagulant was added, the zeta potential of the dye wastewater approached the isoelectric point. This result indicated that the flocs were not influenced by the charge interactions between them. Subsequently, floc adsorption, net sweeping, and micelle adsorption of organic matter may occur. The solution potential gradually increased with the increase in the dosage of the PSAS coagulant. At a PSAS coagulant dose of 200 mg L^{-1}, the solution potential was

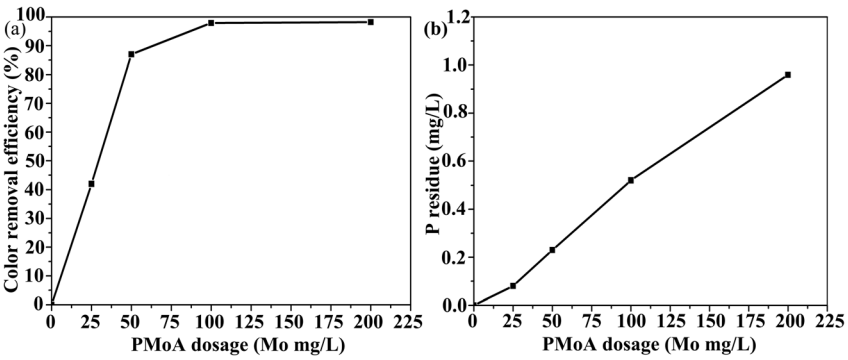

Fig. 5 (a) Effect of PMoA auxiliary dosage on the decolorization of the basic violet 10-simulated wastewater (with a PSAS coagulant) and (b) residual concentration of P in the solution after the coagulation of the dye wastewater.

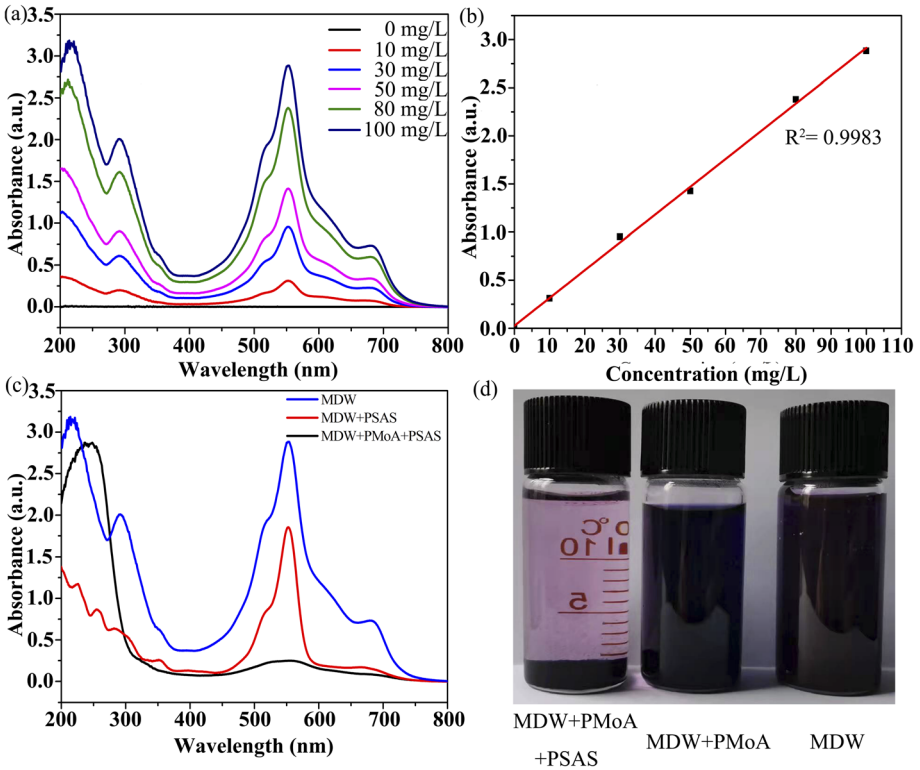

Fig. 6 (a) Absorbance curves of different concentrations of mixed dyes, (b) absorption peak fitting curve at 553 nm for different concentrations of mixed dyes, (c) absorbance change curves before and after coagulations and (d) macroscopic phenomena before and after decolorization.

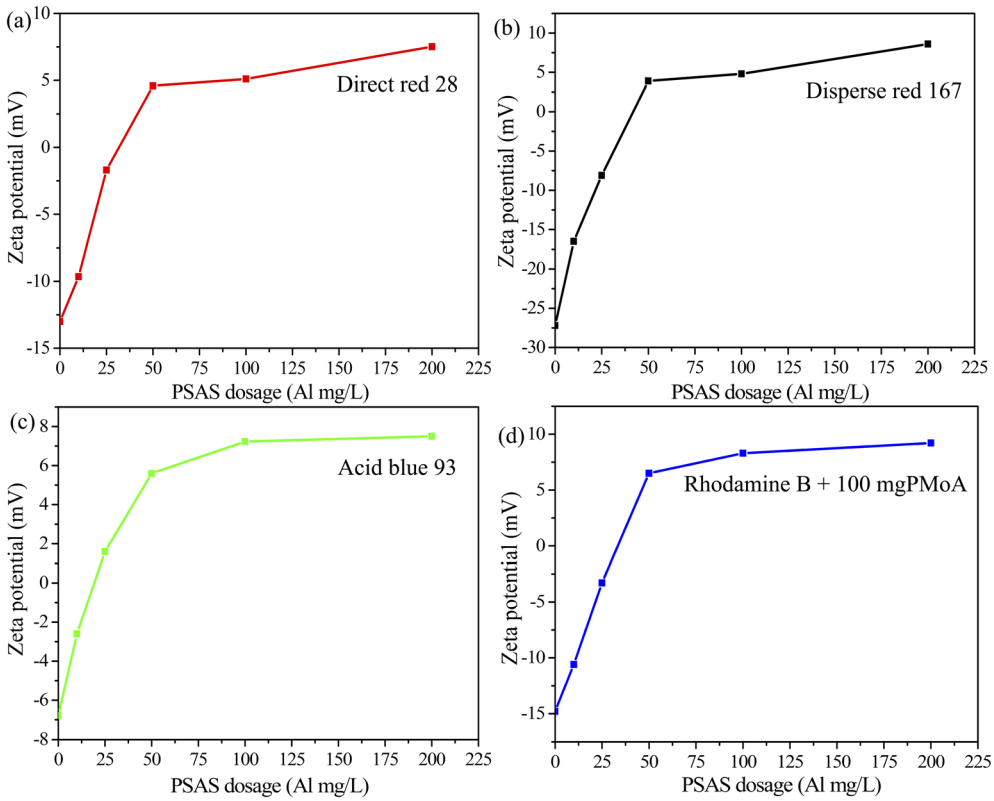

Fig. 7 The effect of the coagulant dosage on the zeta potential: (a) direct red 28 (Congo red), (b) disperse red 167, (c) acid blue 93 and (d) PMoA-basic violet 10 (rhodamine B).

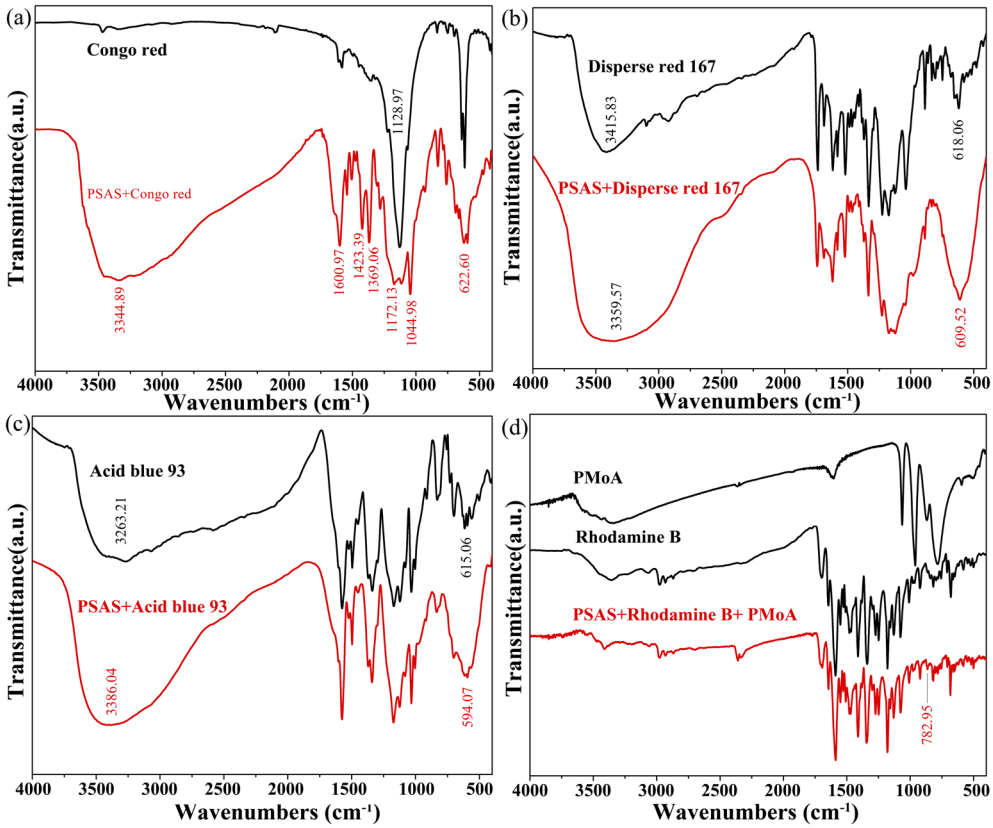

Fig. 8 FTIR spectra of the flocs produced by the PSAS coagulant before and after the adsorption of (a) direct red 28 (Congo red), (b) disperse red 167, (c) acid blue 93 and (d) PMoA-basic violet 10 (rhodamine B).

7.52 mV. Although disperse red dye 167 is a non-ionic dye, the initial potential was −27.2 mV, as shown by the zeta potential measurements. The removal of this dye was attributed to electro-neutralization and net flocculation. Coagulation experiments demonstrated that the inorganic polymer coagulant outperformed other coagulants. For acid blue 93, which has a triarylmethane structure, PSAS flocculates it similarly to direct dyes by binding the positively charged aluminum polymer to the R–SO_3^- structure.[25] At an initial pH of 9, the zeta potential of alkaline rose extract B was −14.33 mV after the addition of 100 mg of PMoA. The subsequent addition of the PSAS coagulant resulted in an increasingly positive solution potential as the coagulant dose increased. This coagulation process was also based on the charge-neutralization effect. The zeta potential test results showed that PSAS had a wide coagulant potential range from −2.3 mV to 9.58 mV.

Fig. 8 shows the infrared spectra of the flocs obtained after treating different dye wastewater with the PSAS coagulant. A comparison before and after coagulation indicated significant changes in the molecular structure of the dye. In the flocs treated with Congo red dye, a broad absorption band was clearly visible at 3344.89 cm^{-1}. This –O–H structure was thought to be related to the Al polymer during the PSAS treatment, as shown in Fig. 8(a).[27] The absorption peak at 1659.85 cm^{-1} was associated with the H–O–H stretching vibration of water. The bending vibration of the R–SO_2–O– structure in Congo red dye appeared at 1128.97 cm^{-1}. In the flocs, the peak of this structure was not very pronounced, implying that the aluminum polymer was bound to the structure. Moreover, as shown in Fig. 8(a–c), the vibrational peaks at 622.6–594.07 cm^{-1} for the Al–O structure indicated that the coagulants interacted with non-basic dyes through oxygen bridge bonds.[28] The IR spectra of PMoA, basic violet 10, and their flocs are shown in Fig. 8(d). The IR spectrum of the flocs resulted from the superposition of the PMoA and basic violet 10 spectra. PSAS likely acted as an acid and

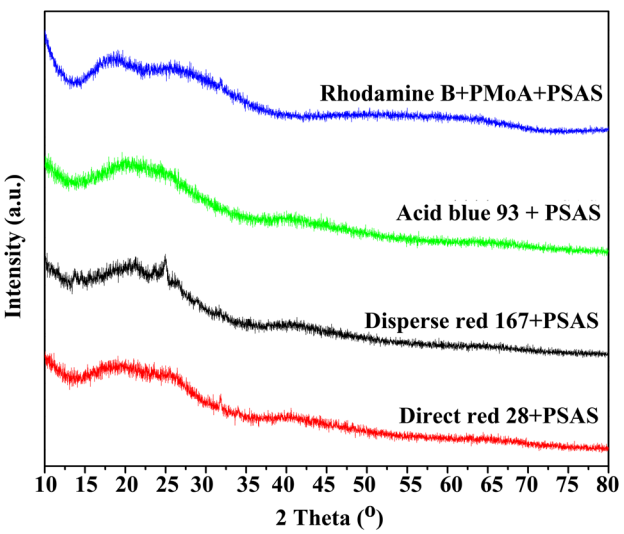

Fig. 9 XRD patterns of the flocs produced by the dyes and the PSAS coagulant.

encapsulated the small flocs. The results indicated that PMoA combined with basic violet 10 to form ionic conjugates, which were then removed using PSAS.

The XRD diffraction patterns of the flocs produced by the combination of PSAS and dye molecules are shown in Fig. 9. Phase analysis indicated that the resulting flocs had no obvious crystalline phase, which was attributed to the disordered structure of PSAS. In coagulation, the treatment technology combines physical and chemical processes. In the first stage, positively charged polymeric aluminum ions and anionic dyes with negatively charged groups undergo an electrical neutralization reaction. At this point, the small flocculent reaches the isoelectric point. However, the formation of large flocs requires external forces or their intrinsic motion. Therefore, effective collisions generated by Brownian motion (perikinetic flocculation) and rapid agitation (orthokinetic flocculation) facilitate particle aggregation.[29] The latter mechanism is considered the primary one. Subsequently, related effects, such as exclusive adsorption coalescence, floc sweep flocculation, or particle cluster adsorption flocculation, may be induced.[30] This process leads to the disorderly agglomeration of flocs rather than orderly growth. Consequently, the flocs exhibited a non-crystalline structure in the XRD pattern.

Based on the systematic performance comparison and characterization of flocs, the interaction mechanisms between PSAS and the different dye groups could be elucidated as follows. For anionic dyes, the dominant mechanism was charge neutralization, followed by specific chemical complexation between the hydrolysates of PSAS and the sulfonate groups (R–SO_3^-) of the dyes,[31] as evidenced by the zeta potential shift to the isoelectric point (Fig. 7a and c) and the significant weakening of the S=O vibration in their FTIR spectra (Fig. 8a and c). For the non-ionic disperse dye, removal primarily occurred through adsorption and sweep flocculation within the amorphous $Al(OH)_3$ precipitates formed at a high pH,[32] as supported by the charge neutralization observed in Fig. 7(b). In contrast, cationic (basic) dyes were not removed by PSAS alone due to electrostatic repulsion between the positively charged dye molecules and PSAS hydrolysates.[33] This critical limitation was overcome by the synergistic PMoA–PSAS system, which operated *via* a two-step mechanism: first, the anionic PMoA complexed with the cationic dye through electrostatic attraction;[34] second, the resulting negatively charged complex was effectively neutralized and enmeshed by PSAS. This synergistic pathway was confirmed by the successful decolorization (Fig. 4c and d), the evolution of the zeta potential (Fig. 7d), and the uniform distribution of Mo and P elements in the flocs (Fig. 11). Therefore, the coagulation mechanism of PSAS was not singular but involved electrostatic neutralization, chemical complexation, or physical enmeshment. The dominant mechanism was dictated by the ionic nature and functional groups of the target dye. The microstructure of the flocculent powder produced by combining PSAS with Congo red, disperse red 167, acid blue 93, and basic violet 10 (with PMoA) was observed using SEM

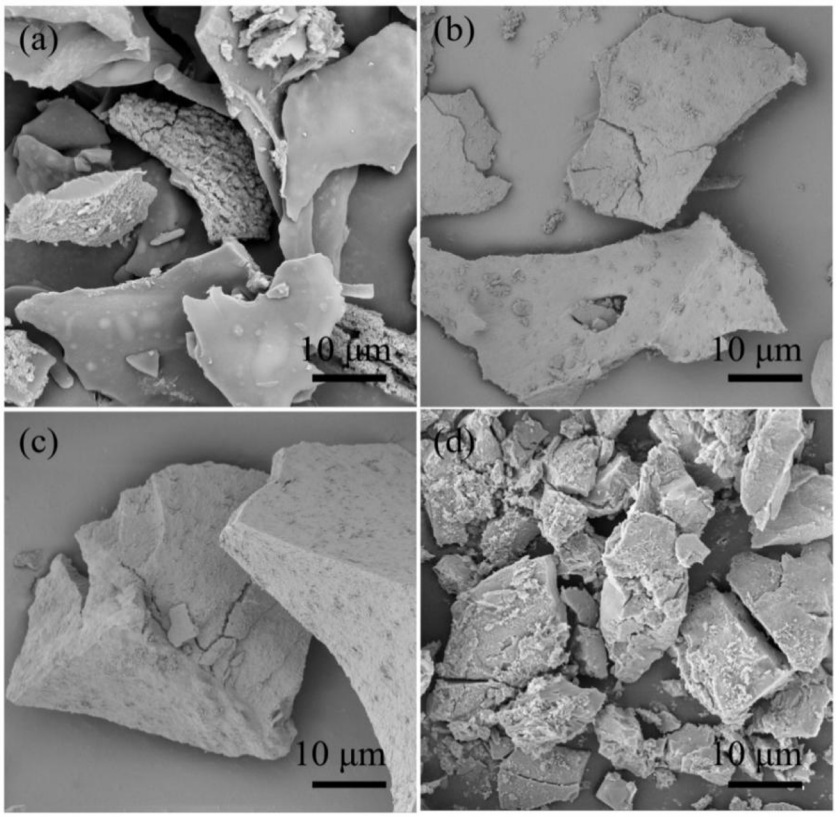

Fig. 10 SEM images of the flocs produced by the dyes and PSAS coagulant: (a) direct red 28 (Congo red), (b) disperse red 167, (c) acid blue 93 and (d) PMoA-basic violet 10 (rhodamine B).

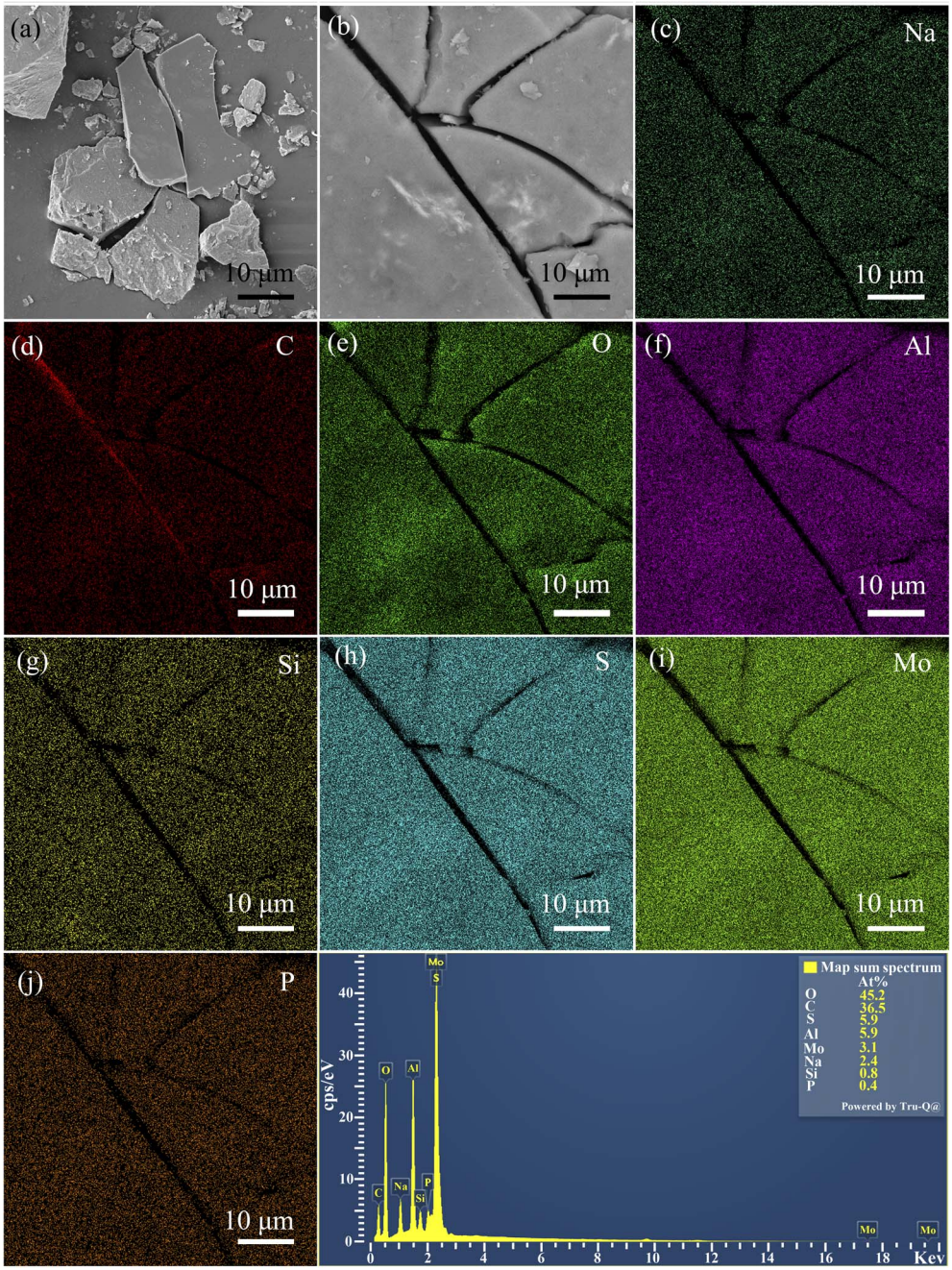

Fig. 11 SEM image of the flocs produced by the mixed dyes and PSAS coagulant, (a) and (b) SEM images; (c–j) elemental mappings: Na, C, O, Al, Si, S, Mo, and P; and (k) EDS patterns.

technology, as shown in Fig. 10. The flocs of PSAS bound to dyes were primarily composed of flakes and blocks. The floc sizes ranged from 10 μm to 100 μm, with a generally large overall particle size. The relatively dense binding and large particles of the flocs facilitated rapid settling, which was advantageous for the PSAS treatment of dye wastewater.

The microscopic morphology of the flocs produced by treating mixed dye wastewater is shown in Fig. 11. A noteworthy result was that the addition of PMoA did not reduce the size of the formed flocs. Therefore, PMoA is feasible as an auxiliary agent for the treatment of mixed dyes. Elemental mapping analysis was further performed to understand the process of combined PSAS and PMoA treatment of mixed dyes, as shown in Fig. 11c–j. The figure showed that elements C, S, Al, O, Mo, P, and Si were uniformly distributed on the surface of the floc. Fig. 11k shows the energy spectrum of the mixed dye flocs, indicating that Mo and S produce the strongest energy peaks, resulting from the superposition of their energies. The content of the corresponding elements is given in the small inset of Fig. 11k. The finding implied that the dye molecules, PMoA, and PSAS were held tightly together, promoting effective removal.

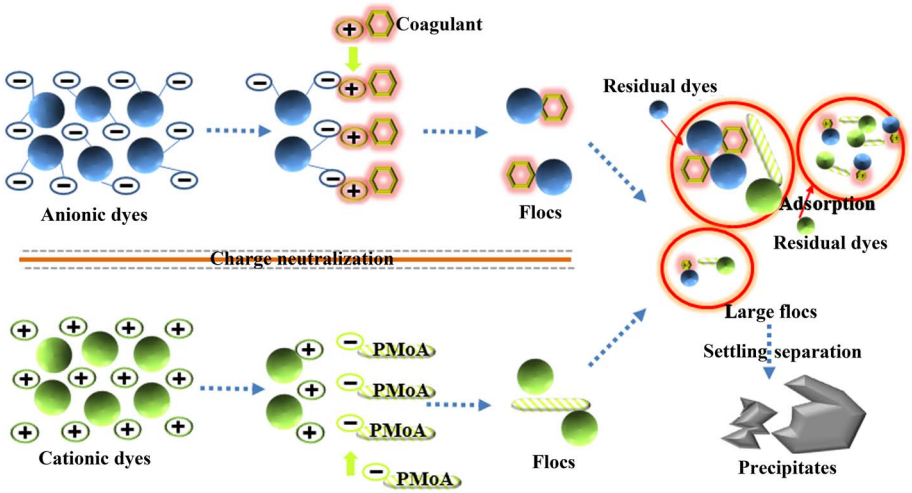

Fig. 12 Scheme of the mechanism of the coagulation process that occurred using PSAS with PMoA.

To clearly comprehend the mechanism of using PSAS coagulation and PMoA in the treatment of mixed dyes, a detailed coagulation process is shown in Fig. 12. Based on the above potential analysis, both anionic and nonionic dye (disperse red 167) wastewater showed a negative charge at a pH of 11. First, charge neutralization played a dominant role. Specifically, the positively charged PSAS formed an electrically neutral polymer with the negatively charged dye. At this stage, the coagulation process involved rapid mixing. The perikinetic coagulation effect induced by the rapid mixing was greater than the orthokinetic effect.[29] The flocs aggregated through bonding and other effects. To prevent large particles from breaking up, the coagulation process involved slow stirring to ensure an adequate reaction (charge neutralization between the dye molecules and PSAS coagulant). In this process, floc sweep coagulation and particle cluster adsorption coagulation further increased the floc size.[22] For cationic dyes, since PMoA was added to the mixed dye before PSAS, the cationic dyes preferentially bonded to PMoA. However, the overall process remained essentially the same. Relevant literature indicates that PMoA has a strong negative charge under acidic conditions.[35] Subsequently, gravity settling-Brownian motion or adsorption-gravity settling occurred in succession during the settling process, effectively removing the dye wastewater.

4. Conclusions

In summary, inorganic polymer coagulants, specifically PAC and PSAS, exhibited superior performances in comparative decolorization studies involving seven coagulants and nine dyes. Notably, the PSAS coagulant demonstrated effectiveness within a pH range of 5–11, with optimal color removal observed at a pH of 11. Efficient decolorization rates of 98.4%, 97.2%, 96.8%, 95.44%, and 91.39% were demonstrated for Congo red, disperse red 167, direct lake blue 5B, acid blue 93, and acid red 27, respectively. However, the decolorization rates for reactive black 5 and reactive blue 21 were relatively poor (40.87% and 75%, respectively). In contrast, for the removal of alkaline dyes, phosphomolybdic acid (PMoA) stood out as the most effective auxiliary agent. The removal efficiency of basic violet 10 reached 94.2% at a pH of 9, with a dosage of 100 mg L^{-1} for PMoA and 50 mg L^{-1} (in terms of Al mg L^{-1}) for the PSAS coagulant. Moreover, the residual phosphorus content in the solution was 0.52 mg L^{-1}, which is below the 1 mg L^{-1} standard specified by China's textile dyeing and finishing industry water pollutant discharge regulation (GB4287-2012). The initial color removal rate for the mixed wastewater (nine dyes) using PSAS was only 25.3%, but this was substantially enhanced to 92.5% upon the addition of PMoA as an auxiliary agent. Further confirmation of the coagulant mechanism of PSAS for dye wastewater treatment was obtained through zeta-potential characterization, revealing a primary charge-neutralizing action. The analysis of the flocs produced by PSAS interacting with dyes showed that the positively charged Al polymer interacted with the negatively charged R–SO_3^- group.

Author contributions

Jie Min: data curation, writing – original draft, writing – review & editing. Huilan Zhou: investigation, conceptualization. Chao Yang: investigation, resources, conceptualization. Lu Wang: investigation, conceptualization. Jiajun Nie: investigation, conceptualization. Qiang Wang: investigation, conceptualization. Lijun Wang: investigation, conceptualization. Yunlong Zhao: project administration, methodology, supervision, funding acquisition, conceptualization.

Conflicts of interest

There are no conflicts to declare.

Data availability

The data that support the findings of this study are available from the corresponding author upon reasonable request.

Acknowledgements

This research was financially supported by the Key Research and Development Projects of Xinjiang Uygur Autonomous Region No. 2024B01018 and the Xinjiang Uygur Autonomous Region Tianchi Talent Young Doctor Introduction Talent Plan Program (Research on the Preparation of Bimetallic Oxide Catalysts and Oxidative Desulfurization Technology for Oil Products) and the Tianshan Talent Research Science and Technology Innovation of Xinjiang Uygur Autonomous Region No. 2024TSYCCX0005.

References

1 J. Abdi, M. Vossoughi, N. M. Mahmoodi and I. Alemzadeh, Synthesis of metal-organic framework hybrid nanocomposites based on GO and CNT with high adsorption capacity for dye removal, *Chem. Eng. J.*, 2017, **326**, 1145–1158.

2 V. Katheresan, J. Kansedo and S. Y. Lau, Efficiency of various recent wastewater dye removal methods: A review, *J. Environ. Chem. Eng.*, 2018, **6**, 4676–4697.

3 Q. Feng, B. Gao, Q. Yue and K. Guo, Flocculation performance of papermaking sludge-based flocculants in different dye wastewater treatment: Comparison with commercial lignin and coagulants, *Chemosphere*, 2021, **262**, 128416.

4 C. R. Holkar, A. J. Jadhav, D. V. Pinjari, N. M. Mahamuni and A. B. Pandit, A critical review on textile wastewater treatments: Possible approaches, *J. Environ. Manage.*, 2016, **182**, 351–366.

5 C. D. Raman and S. Kanmani, Decolorization of Mono Azo Dye and Textile Wastewater using Nano Iron Particles, *Environ. Prog. Sustainable Energy*, 2019, **38**, S366–S376.

6 H. E. Cainglet, T. Saavedra, S. Bürgmayr, J. Zhang, Z. Xie, G. Garnier and J. Tanner, Recycled paper mill process water pre-treatment using ultrafiltration for water system closure, *J. Water Process. Eng.*, 2021, **44**, 102407.

7 F. Amutova, S. Jurjanz, N. Akhmetsadykov, M. Kazankapova, A. Razafitianamaharavo, A. Renard, M. Nurseitova, G. Konuspayeva and M. Delannoy, Adsorption of organochlorinated pesticides: Adsorption kinetic and adsorption isotherm study, *Results Eng.*, 2023, **17**, 100823.

8 Z. Xiong, L. L. Zhang, J. Ma and X. S. Zhao, Photocatalytic degradation of dyes over graphene–gold nanocomposites under visible light irradiation, *Chem. Commun.*, 2010, **46**, 6099–6101.

9 J. Joseph, R. C. Radhakrishnan, J. K. Johnson, S. P. Joy and J. Thomas, Ion-exchange mediated removal of cationic dye-stuffs from water using ammonium phosphomolybdate, *Mater. Chem. Phys.*, 2020, **242**, 122488.

10 Z. Ma, H. Chang, Y. Liang, Y. Meng, L. Ren and H. Liang, Research progress and trends on state-of-the-art membrane technologies in textile wastewater treatment, *Sep. Purif. Technol.*, 2024, **333**, 125853.

11 C. X.-H. Su, L. W. Low, T. T. Teng and Y. S. Wong, Combination and hybridisation of treatments in dye wastewater treatment: A review, *J. Environ. Chem. Eng.*, 2016, **4**, 3618–3631.

12 L. Wang, Z. Lei, S. Yun, X. Yang and R. Chen, Quantitative structure-biotransformation relationships of organic micropollutants in aerobic and anaerobic wastewater treatments, *Sci. Total Environ.*, 2024, **912**, 169170.

13 A. Šuligoj, A. Ristić, G. Dražić, A. Pintar, N. Z. Logar and N. N. Tušar, Bimetal Cu-Mn porous silica-supported catalyst for Fenton-like degradation of organic dyes in wastewater at neutral pH, *Catal. Today*, 2020, **358**, 270–277.

14 X. Luo, C. Liang and Y. Hu, Comparison of Different Enhanced Coagulation Methods for Azo Dye Removal from Wastewater, *Sustainability*, 2019, **11**, 4760.

15 H. Li, S. Liu, J. Zhao and N. Feng, Removal of reactive dyes from wastewater assisted with kaolin clay by magnesium hydroxide coagulation process, *Colloids Surf., A*, 2016, **494**, 222–227.

16 E. Bazrafshan, M. R. Alipour and A. H. Mahvi, Textile wastewater treatment by application of combined chemical coagulation, electrocoagulation, and adsorption processes, *Desalin. Water Treat.*, 2016, **57**, 9203–9215.

17 T. Gupta, J. Cho and J. Prakash, Hydrothermal synthesis of TiO2 nanorods: formation chemistry, growth mechanism, and tailoring of surface properties for photocatalytic activities, *Mater. Today Chem.*, 2021, **20**, 100428.

18 A. Prathan, J. Sanglao, T. Wang, C. Bhoomanee, P. Ruankham, A. Gardchareon and D. Wongratanaphisan, Controlled Structure and Growth Mechanism behind Hydrothermal Growth of TiO2 Nanorods, *Sci. Rep.*, 2020, **10**, 8065.

19 F. Medrano-Rodríguez, A. Picos-Benítez, E. Brillas, E. R. Bandala, T. Pérez and J. M. Peralta-Hernández, Electrochemical advanced oxidation discoloration and removal of three brown diazo dyes used in the tannery industry, *J. Electroanal. Chem.*, 2020, **873**, 114360.

20 Y. Wei, A. Ding, L. Dong, Y. Tang, F. Yu and X. Dong, Characterisation and coagulation performance of an inorganic coagulant—poly-magnesium-silicate-chloride in treatment of simulated dyeing wastewater, *Colloids Surf., A*, 2015, **470**, 137–141.

21 A. Yadav, S. Mukherji and A. Garg, Removal of Chemical Oxygen Demand and Color from Simulated Textile Wastewater Using a Combination of Chemical/Physicochemical Processes, *Ind. Eng. Chem. Res.*, 2013, **52**, 10063–10071.

22 F. Mcyotto, Q. Wei, D. K. Macharia, M. Huang, C. Shen and C. W. Chow, Effect of dye structure on color removal efficiency by coagulation, *Chem. Eng. J.*, 2021, **405**, 126674.

23 K. E. Lee, M. M. Hanafiah, A. A. Halim and M. H. Mahmud, Primary Treatment of Dye Wastewater Using Aloe Vera-aided Aluminium and Magnesium Hybrid Coagulants, *Procedia Environ. Sci.*, 2015, **30**, 56–61.

24 Z. Yang, M. Li, M. Yu, J. Huang, H. Xu, Y. Zhou, P. Song and R. Xu, A novel approach for methylene blue removal by calcium dodecyl sulfate enhanced precipitation and microbial flocculant GA1 flocculation, *Chem. Eng. J.*, 2016, **303**, 1–13.

25 Y. Zhao, Y. Zheng, Y. Peng, H. He and Z. Sun, Characteristics of poly-silicate aluminum sulfate prepared by sol method and its application in Congo red dye wastewater treatment, *RSC Adv.*, 2021, **11**, 38208–38218.
26 P. C. Nnaji, V. C. Anadebe, I. G. Ezemagu and O. Onukwuli, Potential of Luffa cylindrica seed as coagulation-flocculation (CF) agent for the treatment of dye wastewater: Kinetic, mass transfer, optimization and CF adsorption studies, *Arabian J. Chem.*, 2022, **15**, 103629.
27 L. Liu, C. Wu, Y. Chen and H. Wang, Preparation, characterization and coagulation behaviour of polyferric magnesium silicate (PFMSi) coagulant, *Water Sci. Technol.*, 2017, **75**, 1961–1970.
28 Y. Wei, Q. Ji, L. Chen, J. Hao, C. Yao and X. Dong, Preparation of an inorganic coagulant-polysilicate–magnesium for dyeing wastewater treatment: Effect of acid medium on the characterization and coagulation performance, *J. Taiwan Inst. Chem. Eng.*, 2017, **72**, 142–148.
29 H. Holthoff, A. Schmitt, A. Fernández-Barbero, M. Borkovec, M. á. Cabrerízo-Vílchez, P. Schurtenberger and R. Hidalgo-álvarez, Measurement of Absolute Coagulation Rate Constants for Colloidal Particles: Comparison of Single and Multiparticle Light Scattering Techniques, *J. Colloid Interface Sci.*, 1997, **192**, 463–470.
30 M. Khellouf, R. Chemini, Z. Salem, M. Khodja, D. Zeriri and A. Jada, A new activated carbon prepared from cypress cones and its application in the COD reduction and colour removal from industrial textile effluent, *Environment, Development and Sustainability*, 2021, **23**, 7756–7771.
31 E. Guibal, M. van Vooren, B. Dempsey and J. Roussy, A Review of the Use of Chitosan for the Removal of Particulate and Dissolved Contaminants, *Sep. Sci. Technol.*, 2006, **41**, 2487–2514.
32 L. C. Shen and N. P. Hankins, Metallic anion removal from dilute aqueous solutions using polymer-surfactant aggregate process: Effect of surfactant chain length, *J. Water Process. Eng.*, 2017, **20**, 243–248.
33 Z. Mulushewa, W. T. Dinbore and Y. Ayele, Removal of methylene blue from textile waste water using kaolin and zeolite-x synthesized from Ethiopian kaolin, *Environ. Anal. Health Toxicol.*, 2021, **36**, e2021007.
34 J. K. Fink, *Reactive Polymers Fundamentals and Applications: A Concise Guide to Industrial Polymers*, 2nd edn, 2013, pp. 317–330.
35 B. Song, X. Chi, M. Zhou, F. Li, T. Li, J. Wei, O. Donghong and D. Zhang, Enhanced adsorption and dye separation ability of low-cost sepiolite acidified by polyoxometalate acid, *J. Iran. Chem. Soc.*, 2022, **19**, 1457–1465.